

oxyquinoline precipitate was converted into molybdc oxide and placed on the focal circle to cover a wave-length region from 0.74Å to 0.62Å. This chemical procedure is desirable because deuteron bombardment of molybdenum yields a number of masurium activities. Among these is a two-day body which strongly emits molybdenum radiation probably as a result of electron capture.

I wish to thank R. M. Bozorth and the Bell Telephone Laboratories for the gift of a rocksalt crystal and Dr. L. W. Alvarez and Dr. E. Segrè for their advice and suggestions. I wish especially to thank Professor E. O. Lawrence, under whose direction this work was carried out, and the Research Corporation for financial support.

OCTOBER 15, 1939

PHYSICAL REVIEW

VOLUME 56

### On the Single Crystal X-Ray Diffraction Pattern of Calcite

FRANKLIN MILLER, JR.\*

*Ryerson Physical Laboratory, University of Chicago, Chicago, Illinois*

(Received August 17, 1939)

The method of analysis of double spectrometer rocking curves developed by L. P. Smith is reconsidered. Although from Smith's very general viewpoint, six experimental curves are needed for a complete analysis, it is shown that for rocking curves from calcite, taken with the usual type of double spectrometer, it should be possible to deduce the shape of the single crystal diffraction pattern from two rocking curves, the (1,+1) and (2,+2). A method of modifying the equations of the instrument to allow for a simple type of mosaic structure is indicated.

The equations have been applied to rocking curves of  $\text{Mo K}\alpha_1$  from calcite, supplied by L. G. Parratt. The method requires resolution of the observed curves into Fourier components, and a numerical method of doing

this is described. The reliability of the components obtained can be tested by predicting the (1,-1) curve with them and comparing with experiment. In this way it is found that the curves are consistent as regards Fourier components of long period and large amplitude, but inconsistent in the short period, small amplitude components. A single crystal pattern is deduced, based mainly on the observed (1,-1) curve, with asymmetry as indicated by the (1,+1) and (2,+2) curves. It indicates that the crystals used do not have the flat-topped Darwin-Ewald-Prins diffraction pattern. Possible causes of the short period discrepancy have been investigated, but an adequate explanation has not been found.

#### INTRODUCTION

THE object of this work is to determine, from observed two-crystal spectrometer rocking curves, the shape of the single crystal x-ray diffraction pattern applicable to a certain pair of calcite crystals. This function,  $g(\theta)$ , represents the fraction of the incident intensity of a beam of parallel, monochromatic x-rays which is reflected by the crystal when incident at a glancing angle differing by  $\theta$  from the corrected Bragg angle. Knowledge of  $g(\theta)$  is desirable for two reasons. First, a comparison may be made with the Darwin-Ewald-Prins<sup>1</sup> theory. Such a comparison should shed valuable light on the nature of the

imperfection of an almost-perfect crystal. Second,  $g(\theta)$  may be applied as a correction to measured wave-length distributions. Because  $g(\theta)$  has a finite width, an observed emission line, absorption edge, etc., is always distorted by the crystals. Data such as those of Parratt<sup>2</sup> show that the distortion is not a simple process, and knowledge of the entire shape of the diffraction pattern is therefore needed to make the correction. Although for many purposes crystals may be found, such as etched quartz, which possess adequate<sup>3</sup> resolving power in the second or even the first order, occasions arise when, because of intensity difficulties, imperfect crystals must be used. An example is the use of the two-crystal spectrometer as an approximate

\* Now at Rutgers University.

<sup>1</sup> C. G. Darwin, *Phil. Mag.* **27**, 325 and 675 (1914); P. P. Ewald, *Ann. d. Physik* **54**, 519 (1917), *Zeits. f. Physik* **2**, 232 (1920), *Physik. Zeits.* **26**, 29 (1925); J. A. Prins, *Zeits. f. Physik* **63**, 477 (1930).

<sup>2</sup> L. G. Parratt, *Rev. Sci. Inst.* **6**, 387 (1935).

<sup>3</sup> L. G. Parratt, *Phys. Rev.* **46**, 749 (1934).

monochromator. Furthermore, for long wave-length work, relatively imperfect crystals of large grating space must be used.

Previous experimental study of the problem by Allison,<sup>4</sup> Parratt,<sup>5</sup> Renninger,<sup>6</sup> and others has been indirect. Observed values for the parallel position rocking curve width, percent reflection, and coefficient of reflection were compared with predictions of the Prins theory, for various crystals and wave-lengths. For a certain pair of calcites, Parratt and Miller<sup>7</sup> found fairly good agreement at long wave-lengths, but at  $\lambda=0.71\text{\AA}$  the percent reflection was much too small, and the  $(1, -1)$  width too great. An advance was made when L. P. Smith<sup>8</sup> pointed out the power of the Fourier transform method for the problems of the two-crystal spectrometer, and much of the work in this paper is based upon his analysis. Smith showed that the true wave-length distribution of an x-ray line, edge, etc., can be found from proper combination of six observed curves. His quite general treatment does not require specular reflection of each ray from the crystal face. As a result, the definition of  $g(\theta)$  given above has no meaning; nevertheless functions closely related to the diffraction patterns of the two crystals, assumed different, could be found. No application was made to observed curves.

In this paper, simplifying assumptions, applicable to actual calcite specimens, are made in Smith's analysis, and the effects of a simple type of mosaic structure and of vertical divergence are included. It turns out that  $g(\theta)$  can be found from two observed curves, the  $(2, +2)$  curve being to a sufficient approximation the true line shape. Mosaic structure is introduced as follows: The crystal face is assumed to be covered by blocks which are large enough (say,  $10^{-4}$  cm on an edge) so that no radiation completely traverses a block, and diffraction effects due to the finite number of planes in a block can be ignored. The function  $g(\theta)$  is considered applicable to each block. A parallel incident beam is then reflected from the crystal face as a divergent beam, although specular reflection is assumed for each block. The amount of divergence depends on the

probability distribution function for orientation of the blocks; by letting the distribution function become infinitely sharp we pass to the case of a perfect crystal.

#### MATHEMATICAL THEORY

Following Smith, we will denote by upper case symbols the Fourier transforms of functions denoted by corresponding lower case symbols. Thus

$$\text{if } F(t) = \text{const.} \times \int_{-\infty}^{\infty} f(x) e^{itx} dx, \quad (1)$$

$$\text{then } f(x) = \text{const.} \times \int_{-\infty}^{\infty} F(t) e^{-ixt} dt. \quad (2)$$

The broad restrictions on  $f(x)$  required for this inversion to be possible are fulfilled for the functions under consideration. We will also have use for a transform of the type

$$\mathfrak{F}(t) = \text{const.} \times \int_{-\infty}^{\infty} f(x) e^{itx^2} dx, \quad (3)$$

which may be called a Fresnel transform, denoted by corresponding script symbols.

For each of the three observed rocking curves an integral equation can be set up and the Fourier transform written down. The angles involved are illustrated for a parallel position in Fig. 1; the derivation of Eqs. (4) to (7) follows the general scheme of Chapter IX of *X-Rays in Theory and Experiment*, by Compton and Allison.<sup>9</sup> It is assumed that both crystals are rotated by equal amounts in recording the curves. By this method

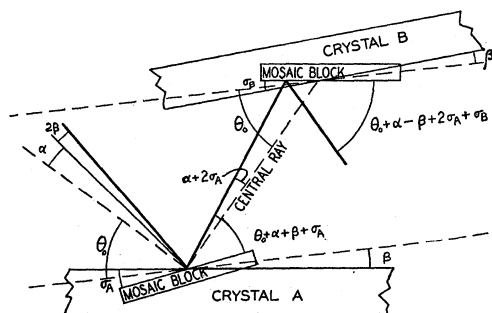


FIG. 1. Crystal arrangement in a parallel position.

<sup>4</sup> S. K. Allison, Phys. Rev. **41**, 1 (1932).

<sup>5</sup> L. G. Parratt, Phys. Rev. **41**, 561 (1932).

<sup>6</sup> M. Renninger, Zeits. f. Krist. **89**, 344 (1934).

<sup>7</sup> L. G. Parratt and F. Miller, Phys. Rev. **49**, 280 (1936).

<sup>8</sup> L. P. Smith, Phys. Rev. **46**, 343 (1934).

<sup>9</sup> A. H. Compton and S. K. Allison, *X-Rays in Theory and Experiment* (D. Van Nostrand Co., 1935). References are there given to contributions of Schwarzschild, Spencer, Laue, and others to the theory of the instrument.

of "double rotation"<sup>10, 11</sup> the effect of inhomogeneity in the focal spot or the crystal surfaces is almost completely eliminated. It must be remembered that if each crystal is rotated by an amount  $\beta$  about its own axis, either the x-ray tube must be rotated by  $2\beta$  or crystal  $B$  must be rotated about crystal  $A$ , in order for the effective beam from the center of the focal spot to strike the same regions of the crystals. The two cases are identical mathematically, and the former is assumed in drawing Fig. 1. Vertical divergences, and vertical deviations of the mosaic blocks, are not shown in Fig. 1, and it is due to these that terms involving  $\phi$  and  $\psi$  are introduced into the arguments of the  $g$  functions by considerations similar to those accompanying Fig. IX-11 of reference 9. The terms in  $\xi$ , which is a wave-length variable, recognize the fact that, according to the Bragg law, change in wave-length of an elementary ray can compensate for a change in the glancing angle introduced, say, by horizontal divergence. The nomenclature and resulting equations may easily be extended to positions  $(n_1, \pm n_2)$ , where  $n_1 \neq n_2$ .

For an  $(n, -n)$  curve, we obtain from Fig. 1 the equation

$$\begin{aligned}
 p_n(\beta) = \text{const.} \times & \int_{-\infty}^{\infty} \int_{-\infty}^{\infty} \int_{-\infty}^{\infty} \int_{-\infty}^{\infty} \int_{-\infty}^{\infty} \int_{-\infty}^{\infty} m(\alpha) s(\phi) \\
 & \times j(\xi) f(\sigma_A) f(\sigma_B) f(\psi_A) f(\psi_B) \\
 & \times g_A(\beta + \alpha + \sigma_A - a_n \psi_A^2 - a_n \phi^2 - a_n \xi) \\
 & \times g_B(-\beta + \alpha + 2\sigma_A + \sigma_B \\
 & - 2a_n \psi_A^2 - a_n \psi_B^2 - a_n \phi^2 - a_n \xi) \\
 & \times d\alpha d\phi d\xi d\sigma_A d\sigma_B d\psi_A d\psi_B. \quad (4)
 \end{aligned}$$

$\beta$  = deviation of crystal  $B$  from the central position in which the glancing angle of the central ray is  $\theta_0$ .

$\alpha$  = horizontal divergence of a ray from the central ray.

$\phi$  = vertical divergence of a ray from the central ray.

$\sigma_A, \sigma_B$  = horizontal deviations of mosaic blocks from the cleavage plane.

$\psi_A, \psi_B$  = vertical deviations of mosaic blocks from the cleavage plane.

$$a_n = \frac{1}{2} \lambda_0 (\partial \theta_0 / \partial \lambda_0) = \frac{1}{2} \tan \theta_0.$$

<sup>10</sup> J. W. M. DuMond and A. Hoyt, Phys. Rev. **36**, 1702 (1930).

<sup>11</sup> S. K. Allison, Phys. Rev. **44**, 63 (1933).

$$\xi = 2(\lambda - \lambda_0) / \lambda_0.$$

$p_1(\beta)$ ,  $r_1(\beta)$ , and  $r_2(\beta)$  are the  $(1, -1)$ ,  $(1, +1)$ , and  $(2, +2)$  rocking curves, for double rotation.

$m(\alpha)$  and  $s(\phi)$  are slit functions, determined by the geometry of the slits and the focal spot intensity distribution.

$f(\sigma_A)$ , etc., are the mosaic distribution functions postulated in paragraph 3, and assumed similar for the two crystals.

$j(\xi)$  is the true emission line shape.

$g_A(\theta)$  and  $g_B(\theta)$  are the crystal patterns of the two crystals.

The integrations are extended to infinite limits because all of the functions involved become zero sufficiently rapidly.

We must now assume  $m(\alpha)$  to be "very wide" and hence constant over the effective range of  $\alpha$ . This is justified since the rocking curves are only a few seconds wide, whereas the beam defined by the slits and focal spot is many minutes wide.<sup>12</sup>

Upon multiplication of Eq. (4) by  $e^{2it\beta} d\beta$  and integration, the integral splits into 8 single integrals as follows:

$$\begin{aligned}
 & \int_{-\infty}^{\infty} p_n(\beta) \exp(2it\beta) d\beta = \text{const.} \\
 & \times \int_{-\infty}^{\infty} s(\phi) d\phi \int_{-\infty}^{\infty} j(\xi) d\xi \int_{-\infty}^{\infty} f(\sigma_A) \exp(it\sigma_A) d\sigma_A \\
 & \times \int_{-\infty}^{\infty} f(\sigma_B) \exp(it\sigma_B) d\sigma_B \\
 & \times \int_{-\infty}^{\infty} f(\psi_A) \exp(-a_n i t \psi_A^2) d\psi_A \\
 & \times \int_{-\infty}^{\infty} f(\psi_B) \exp(-a_n i t \psi_B^2) d\psi_B \\
 & \times \int_{-\infty}^{\infty} g_A(\beta + \alpha + \sigma_A - a_n \psi_A^2 - a_n \phi^2 - a_n \xi) \\
 & \times \exp[it(\beta + \alpha + \sigma_A - a_n \psi_A^2 - a_n \phi^2 - a_n \xi)] \\
 & \times g_B(-\beta + \alpha + 2\sigma_A + \sigma_B - 2a_n \psi_A^2 \\
 & - a_n \psi_B^2 - a_n \phi^2 - a_n \xi) \exp[it(\beta - \alpha - 2\sigma_A - \sigma_B \\
 & + 2a_n \psi_A^2 + a_n \psi_B^2 + a_n \phi^2 + a_n \xi)] d\alpha d\beta. \quad (5)
 \end{aligned}$$

or

$$P_n(2t) = \text{const.} \times F^2(t) \mathfrak{F}^{*2}(a_n t) G_A(t) G_B^*(t). \quad (6)$$

<sup>12</sup> This assumption is also made by Smith, and is surely valid for an  $(n, -n)$  curve. For an  $(n, +n)$  curve its validity is more certain in double rotation.

The asterisk indicates a complex conjugate. The derivation of Eq. (6) uses the fact that

$$\int \int_{-\infty}^{\infty} f_1(x+y+a)f_2(x-y+b)dx dy = \frac{1}{2} \left[ \int_{-\infty}^{\infty} f_1(x)dx \right] \times \left[ \int_{-\infty}^{\infty} f_2(x)dx \right].$$

For an  $(n, +n)$  curve, (antiparallel position), the equation analogous to Eq. (4) is

$$r_n(\beta) = \int \int \int \int \int \int \int_{-\infty}^{\infty} m(\alpha)s(\phi) \times j(\xi)f(\sigma_A)f(\sigma_B)f(\psi_A)f(\psi_B) \times g_A(\beta+\alpha+\sigma_A-a_n\psi_A^2-a_n\phi^2-a_n\xi) \times g_B(\beta-\alpha-2\sigma_A-\sigma_B-2a_n\psi_A^2-a_n\psi_B^2 - a_n\phi^2-a_n\xi)d\alpha d\phi d\xi d\sigma_A d\sigma_B d\psi_A d\psi_B. \quad (7)$$

This yields

$$R_n(2t) = \text{const.} \times \mathfrak{S}(2a_n t) J(2a_n t) F^2(t) \times \mathfrak{F}(a_n t) \mathfrak{F}(3a_n t) G_A(t) G_B(t). \quad (8)$$

The parameter  $t$  is to be interpreted as the analogue of  $n$  when a periodic function  $f(x)$  is written as a Fourier series  $\sum A_n \cos(nx - \delta)$ . Thus we speak of the " $t$ th" component of a curve. Since our functions are not periodic, the parameter  $t$  has nonintegral values, and  $P_n(2t)$ , etc., are continuous functions of  $t$ .

For the present we will assume the pattern for crystal  $A$  to differ from that for crystal  $B$  only by a constant real factor. The validity of this assumption will be discussed below. Let  $g_1(\theta)$  and  $g_2(\theta)$  denote the single crystal patterns in the first and second orders. From the three experimental curves we get three equations in the parameter  $t$ :

$$(1, -1): P_1(2t) = \text{const.} \times F^2(t) \mathfrak{F}^{*2}(a_1 t) G_1(t) G_1^*(t), \quad (9)$$

$$(1, +1): R_1(2t) = \text{const.} \times \mathfrak{S}(2a_1 t) J(2a_1 t) F^2(t) \mathfrak{F}(a_1 t) \mathfrak{F}(3a_1 t) G_1^2(t), \quad (10)$$

$$(2, +2): R_2(2t) = \text{const.} \times \mathfrak{S}(2a_2 t) J(2a_2 t) F^2(t) \mathfrak{F}(a_2 t) \mathfrak{F}(3a_2 t) G_2^2(t). \quad (11)$$

Elimination of  $J$  from Eqs. (10) and (11) gives

$$G_1^2(t) = \text{const.} \times \frac{R_1(2t)}{R_2(2a_1 t/a_2)} \times \left[ \frac{F^2(a_1 t/a_2)}{F^2(t)} G_2^2(a_1 t/a_2) \right]. \quad (12)$$

Also, we must have

$$|P_1(2t)| \times |R_2(2a_1 t/a_2)| = \text{const.} \times |R_1(2t)| \times |\mathfrak{F}^{*2}(a_1 t) F^2(a_1 t/a_2) G_2^2(a_1 t/a_2)|. \quad (13)$$

Since the effect of  $\mathfrak{F}$  will be small compared with that of  $F$ , and since  $G_2$  can be estimated from the  $(2, -2)$  rocking curve, Eq. (13) offers a method of estimating the mosaic distribution function, and hence of determining the crystal pattern  $g_1(\theta)$  from (12). To a very good approximation, for calcites of ordinary perfection, the expression in brackets in Eq. (12) can be regarded as constant, which amounts to assuming infinite resolving power in the second order and assuming perfect crystals.

It is instructive to discuss a few well-known properties of the instrument from the point of view of the Fourier transforms, Eqs. (9) to (13). No attempt is made to give references to the first discussions in the literature of some of these points. It must be borne in mind that the Fourier transform of a symmetrical function is real, while the Fresnel transform of even a symmetrical function is, in general, complex. Also, a narrow curve has a wide transform, and vice versa, since many high components are required to represent a sharp curve. Thus, in particular, the transform of a witch (Hoyt<sup>13</sup> curve) given by  $1/(1+x^2/a^2)$ , of half-width  $a$ , is proportional to  $e^{-|at|}$ .

(a) If the crystal patterns are identical in shape and there is no mosaic structure, then Eq. (6) shows that  $P_n(2t)$  is real, and all the  $(n, -n)$  curves are symmetrical. The converse is not true, however. If we write  $G_A = G_A' + iG_A''$ , etc., a real  $P_n(2t)$  implies only that  $G_A G_B^*$  is real, i.e.,  $G_A''/G_A' = G_B''/G_B'$ . This can be satisfied in two ways: either  $g_A(\theta)$  is proportional to  $g_B(\theta)$ , and the patterns (in general asymmetrical) have identical shapes, or  $G_A'' = G_B'' = 0$ , in which case the patterns are both symmetrical, but not necessarily alike. The first case has been assumed in deriving Eqs. (9) to (13), since the  $(n, -n)$

<sup>13</sup> A. Hoyt, Phys. Rev. 40, 477 (1932).

curves are always observed to be symmetrical. It can easily be seen that if the second case is true, then Eq. (13) still holds, since then  $G_B^* = G_B$ , and  $G_z^2$  becomes  $(G_2)_A(G_2)_B$ . Mosaic structure would not affect this conclusion, barring a fortuitous coincidence of the odd parts of  $\mathfrak{F}$  and  $G_A G_B^*$ .

(b) If the vertical divergence is negligibly small then  $\mathfrak{S}$  reduces to a constant. Vertical divergence has no effect on an  $(n, -n)$  curve, but since  $\mathfrak{S}(a_n t)$  is not always real, asymmetry will be introduced into an  $(n, +n)$  curve even by a symmetrical slit function.

(c) The effect of mosaic structure will be to widen each curve, since  $F$  and  $\mathfrak{F}$  surely decrease with increasing  $t$  for small  $t$ . Any positive function exhibits such a behavior.

(d) If the true line shape and diffraction pattern are both witches of widths  $w_j$  and  $w_g$ , respectively, then the  $(1, -1)$  curve is a witch of width  $w_p = 2w_g$ , and the  $(1, +1)$  curve is a witch of width  $w_r = w_j + 2w_g = w_j + w_p$ . This follows immediately from the properties of the exponential  $e^{-wt}$ , and the witch is obviously the only function for which the widths add in such a simple manner. Using the Fourier transform method, an observed curve can be corrected for the finite width of the diffraction pattern, by dividing the transform of the observed curve by the square of an assumed or derived single crystal pattern transform. Ordinarily a witch of half the width of the  $(n, -n)$  curve will suffice for this correction. Methods based on assumptions of witches, error curves, etc., have previously been applied only to widths of emission lines.

#### APPLICATION TO ACTUAL CURVES

Three rocking curves were recorded by Professor Parratt for  $\text{MoK}\alpha_1$  at 0.71Å on the direct-reading spectrometer of Richtmyer and Barnes.<sup>14</sup> Maximum vertical divergence was  $4.5 \times 10^{-3}$  radian. Voltage was kept low enough so that radiation of half the wave-length studied was not excited. Background was 0.5 percent in the first order, and 4 percent in the second order. The crystals were  $\text{A}_5\text{B}_5$  of reference 2, after repeated etching and grinding according to the method of Manning.<sup>15</sup> Crystals  $\text{A}_4\text{B}_4$  of reference 2, of which an extended indirect study had already been made,<sup>7</sup> were found to have deteriorated badly since 1935. The percent reflection could be brought only to 40 percent compared with 66 percent in 1935. The crystals used have a percent reflection of 50 percent, and represent the most nearly perfect crystals available after an extended search. While not as nearly perfect as some specimens previously reported, they are

<sup>14</sup> F. K. Richtmyer and S. W. Barnes, Rev. Sci. Inst. **5**, 351 (1934).

<sup>15</sup> K. V. Manning, Rev. Sci. Inst. **5**, 316 (1934).

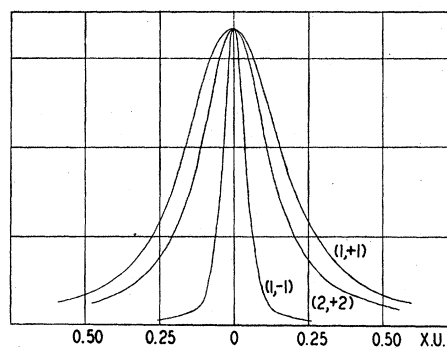


FIG. 2. Rocking curves of  $\text{MoK}\alpha_1$  on calcite, recorded by L. G. Parratt. All of the data for the wings are not plotted.

comparable with crystals commonly used in x-ray spectroscopy.

The observed curves are plotted in Fig. 2. From 70 to 100 ordinates were observed for each curve. The  $(2, +2)$  curve,  $r_2(\beta)$ , was symmetrical, and accurately a witch of full width 0.268 x.u. Such a shape has been observed previously for  $\text{MoK}\alpha_1$ , but is not typical of all lines. It is interesting to observe that both classical<sup>16</sup> and modern<sup>17</sup> theories predict such a shape for an x-ray emission line.<sup>18</sup> The  $(1, +1)$  curve,  $r_1(\beta)$ , of width 0.384 x.u., was not a witch, and showed an extremely slight asymmetry which was probably real. The origin was taken as the intersection with the baseline of the locus of midpoints of horizontal segments; as so defined it differed by only 0.007 x.u. from the location of the peak. The odd part of  $r_1(\beta)$  was thus very small (maximum value 3 percent of the peak) and its effect on  $|R_1|^2 = R_1'^2 + R_1''^2$  was entirely negligible. Correction of the  $(n, +n)$  curves for overlap of  $\text{K}\alpha_2$  was important only for  $r_1(\beta)$ , and was carried out in a direct manner. The overlapping factor<sup>11</sup> was only 0.010 for  $(1, +1)$  and 0.005 for  $(2, +2)$ . The correctness of the procedure was indicated by comparison of the two wings of a curve. No differences were found. The  $(1, -1)$  curve,  $p_1(\beta)$ , was symmetrical, as expected, and had a width of 0.0868 x.u. All of the observed curves were found to decrease as the inverse square for abscissas farther than

<sup>16</sup> N. C. Mandersloot, Jarb. d. Rad. u. Elektrotek. **13**, 16 (1916); G. E. M. Jauncey, Phys. Rev. **19**, 68 (1922).

<sup>17</sup> V. Weisskopf and E. Wigner, Zeits. f. Physik **63**, 54 (1930); F. Hoyt, Phys. Rev. **38**, 860 (1930).

<sup>18</sup> See, however, remarks by A. Hoyt, reference 13.

about two full widths from the peak. E.g., for  $r_2(\beta)$  a least-squares solution using 14 ordinates gave a value of  $-2.0$  for the exponent.

A straightforward numerical method was adopted for the Fourier analysis, after trial showed the rolling sphere Henrici type analyzer to be unsuited to precise determination of short period components. The method of Robertson<sup>19</sup> was modified slightly as follows: A series of 1000 cardboard strips was prepared, each containing the sequence  $N, N \cos 6^\circ, N \cos 12^\circ \dots 0$ , written from top to bottom to the nearest integer. To analyze a curve, ordinates were read off a large graph, spaced  $q$  units apart. Corresponding strips were hung, 15 at a time, on a plywood strip, and the appropriate products  $f(x) \frac{\sin}{\cos} tx$  read through diagonal rows of holes in a cardboard screen. The algebraic sums of the visible numbers were proportional to the real and imaginary parts of  $F(t_0)$ , where  $t_0 = \pi/(30q)$ . By discarding alternate strips and using the remainder again,  $F(\frac{1}{2}t_0), F(\frac{1}{4}t_0)$ , etc., were rapidly obtained. Three selections of ordinates at spacings of, say, 0.002, 0.0025, and 0.003 x.u. sufficed to give about 15 well spaced components,<sup>20</sup> and the area of the curve gave  $F(0)$ . The even and odd parts of a curve were analyzed separately, integration extending from 0 to  $+\infty$ . A formula for

$$\int_N^\infty x^{-n} \cos tx dx,$$

with  $n$  in general not an integer, was developed in such a form that the contributions of the wings to the Fourier components could be easily inserted in the analysis; for  $\cos Nt=1$  and  $Nt \gg 0$ , the integral is  $n/(t^2 N^{n+1})$ . As a check on this numerical method several arbitrary curves, including asymmetrical ones, were broken down into components with the aid of the strips, and then synthesized, also with the strips. Satisfactory agreement, to within about 1 percent, was obtained.

<sup>19</sup> J. M. Robertson, Phil. Mag. 21, 176 (1936).

<sup>20</sup> Robertson's procedure for obtaining higher components amounts to using different screens. This must lead to error for high components; thus a sine component of 30 times the  $t$  value of the fundamental would have arguments spaced  $180^\circ$  apart and would vanish, regardless of the curve being analyzed. In Robertson's application to crystal structure work this is not serious.

## RESULTS AND CONCLUSIONS

In Figs. 3 and 4 are shown the transforms of the three observed curves, plotted logarithmically. The  $t$  values are determined by the angular unit used in plotting the curves, which in this work was 34.29 seconds, corresponding to 1 x.u. in the  $(1, +1)$  position. Since  $p_1(\beta)$  was much narrower than the other two it was possible to be certain of  $P_1(t)$  for much larger  $t$  values. The uncertainties represented by vertical lines indicate twice the total contributions of the wings to the transforms, using the inverse square assumption. This is a very liberal estimate, since the wings were observed to follow this rule out to abscissas much larger than those at which the numerical analyses were stopped. The error introduced by the numerical analysis itself is, for the components plotted, too small to be drawn. The fact that  $r_2(\beta)$  is a good approximation to a witch is shown by the straightness of its transform when plotted in this manner.

In Fig. 4 is plotted also  $\log_{10} |P_1 R_2|$ . If  $F, \mathfrak{F}$ , and  $G_2$  are infinitely sharp, Eq. (13) shows that  $\log |P_1 R_2|$  should be parallel to  $\log |R_1|$ , as in the dashed line. It is seen that there is agreement among the components of long period and large amplitude (small  $t$ ). Although definite disagreement is indicated among the components of short period, the amplitudes of these range from  $1/5$  to  $1/100$  of the most intense amplitudes. Lacking other sets of data, it seems best at present to interpret Fig. 4 as indicating a

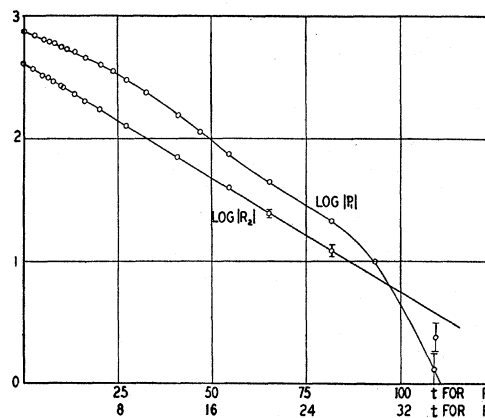


FIG. 3. Fourier transforms of the observed  $(1, -1)$  curve,  $|P_1|$ , and of the observed  $(2, +2)$  curve,  $|R_2|$ . The scale of ordinates is arbitrary.

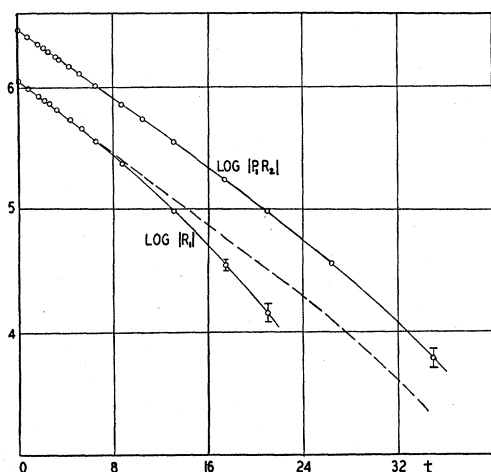


FIG. 4. Upper curve: Product of the curves of Fig. 3. Lower curve: Fourier transform of the observed (1, +1) curve,  $|R_1|$ . The dashed curve is parallel to the upper curve, and should coincide with the lower curve, according to Eq. (13).

general, but not detailed, confirmation of the theory of the double spectrometer.

In order to obtain the single crystal pattern  $g_1(\theta)$ , the most certain procedure is to obtain  $|G_1|$  from the observed (1, -1) curve, using Eq. (9). The (1, +1) and (2, +2) data can then be used to find the ratio of real and imaginary parts of  $G_1(t)$ . Thus  $G_1(t)$ , and hence  $g_1(\theta)$ , are completely determined, and the pattern so found automatically predicts the correct (1, -1) curve. Of course,  $G_1$  could be found directly from the (1, +1) and (2, +2) curves by Eq. (12), but the other method is more accurate since it places reliance upon the curve which is, in width, most nearly like the desired function.

Application of the first method yields curve *A* of Fig. 5. The observed percent reflection of 50 percent served to fix the scale of ordinates. This curve is almost symmetrical, since the (1, +1) curve showed only very slight asymmetry, and the (2, +2) curve none at all. The predicted Prins curve is plotted as *B* of Fig. 5, and is the average for the two kinds of polarization. Such an average is allowable for the small glancing angles involved here. The pattern derived from experiment shows no evidence for the flat top of the Darwin-Ewald-Prins theory. It should be mentioned that Fourier analysis of the (1, -1) curve was carried out to large enough  $t$  values (>500) to make certain that the round top of

Fig. 5*A* is significant, and not due to neglect of higher components.

Curve *A* of Fig. 5 is derived by the most trustworthy method, and represents our best estimate of the single crystal pattern of the crystals used. Nevertheless, too much confidence should not be placed in the derived curve on account of the discrepancy of Fig. 4 among the higher components. That this discrepancy is serious becomes evident when the single crystal pattern is computed directly from the antiparallel curves. The resulting  $g(\theta)$  is over twice as wide as curve *A*, and yields a (1, -1) width of 0.21 x.u. This is unthinkable large compared with the observed 0.087 x.u. The only reasonable explanation is that one, or both, of the observed antiparallel curves has been distorted in some unknown fashion. It is easiest to imagine that the true (1, +1) curve is narrower than that observed; a width of 0.31 x.u. instead of 0.38 would bring about agreement. (This figure was obtained from the slope of the dashed line of Fig. 4, allowing 0.01 x.u. for the (2, -2) width). It should be emphasized, however, that such an arbitrary correction is entirely outside of the observational error.

No adequate explanation for this inconsistency among the higher components has been found. Among the possible reasons for it which have been considered are: (a) Making the correction for finite resolving power in the second order tends to increase the discrepancy, and the correction would be only about a 4 percent change in the slope of the upper line of Fig. 4, in the wrong direction. (b) The effect of the perhaps oversimplified mosaic structure of para-

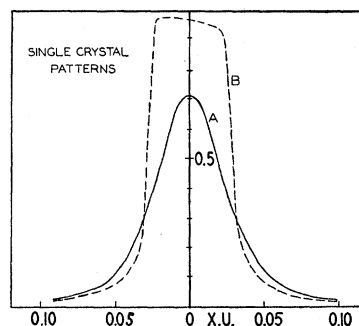


FIG. 5. *A*: Single crystal pattern deduced from the observed rocking curves. *B*: Diffraction pattern predicted by the Prins theory.

graph 3 will also tend to increase the discrepancy, since the mosaic distribution function is surely a positive function, and its transform decreases with increasing  $t$ . Qualitatively, the effect of mosaic structure can be seen as follows: Each of the three curves is widened by about the same amount by such a mosaic structure. Therefore one would expect the observed  $r_1$  to be wider than the true  $r_1$ , but narrower than that predicted from the observed  $p_1$  and  $r_2$ , since both of the latter have been widened. The opposite is observed. (c) The assumption that  $m(\alpha)$  is "very wide" was made in deriving Eqs. (6) and (8). If there is mosaic structure, the effective range of  $\alpha$  will no longer be of the order of the diffraction pattern width, but will be comparable to the width of  $f(\sigma)$ . As mentioned above,  $f(\sigma)$  must be narrow, otherwise the (1, -1) curve would be broadened. Hence the assumption of  $m(\alpha)$  constant is justified. (d) For the slits used, the maximum vertical divergence is so small that at  $t=20$  the function  $\mathfrak{S}(a_1t)$  is still 99.5 percent of its value at  $t=0$ , using a slit function  $s(\phi) = 1 - |\phi/\phi_{\max}|$ . (e) Possible dissimilarity of the two crystals is discussed above. It was shown that the only kind of dissimilarity consistent with the symmetry of the (1, -1) curve would not affect the validity of Eq. (13), on which Fig. 4 is based. (f) Close consideration of the original curves and their treatment rules out explanations in terms of observational or computational error, improper correction for overlapping of  $\text{MoK}\alpha_2$ , or incorrect treatment of the wings.

The essential point of the analysis presented here is that for ordinary calcite crystals the second-order resolving power is so high that only a small, easily estimated correction is needed to obtain the true line shape. In theory, at least, not only the single crystal diffraction pattern can be deduced, but also the distribution function of the mosaic blocks. When the method is applied to L. G. Parratt's precisely recorded rocking curves of  $\text{MoK}\alpha_1$ , a general agreement among the long period Fourier components indicates that the theory of the double spectrometer is not entirely wrong. The serious and definite discrepancy among the short period components, however, is difficult to explain. The conclusion that the single crystal pattern (Fig. 5A) shows no evidence for the flat top of the Darwin-Ewald-Prins theory is valid regardless of this discrepancy, since the doubtful assumption concerns only the asymmetry of the pattern.

#### ACKNOWLEDGMENTS

Sincere thanks are due to Professor Samuel K. Allison, whose continued interest in the theory of the two-crystal spectrometer led to the undertaking of this analysis. The author is deeply indebted to Professor Lyman G. Parratt, who painstakingly recorded the data, and with whom he has had several valuable discussions. Discussions with Professor Frank G. Dunnington, and assistance of Libuse Lukas Miller with the numerical work, were also of value.